



ELSEVIER

Physica C 368 (2002) 320–323

PHYSICA C

www.elsevier.com/locate/physc

# A multi-Josephson junction qubit

S.P. Yukon\*

*Air Force Research Laboratory, Electromagnetics Technology Division, Hanscom, AFB MA 01731, USA*

## Abstract

We have designed a persistent supercurrent multi-Josephson junction (JJ) qubit whose circuit is based on a flattened JJ triangular prism. The Schrödinger equation for the 1D constrained system is equivalent to the Whittaker Hill equation, for which exact solutions have been found [1]. Symmetric or antisymmetric coupling of the qubit to an external magnetic field, will excite only the corresponding symmetric or antisymmetric terms in the Hamiltonian. This specificity allows coupling to a system bus comprised of an LC resonant loop. We indicate how separate buses might be coupled into a larger branching network. Published by Elsevier Science B.V.

*Keywords:* Josephson junction; Qubit; Triangular qubit gate; Control Z gate

## 1. Introduction

The qubit circuit is based on a discretized and flattened version of the triangular long Josephson junction (JJ) prism discussed in Refs. [2–4] and is shown in Fig. 1. The long JJ prism was shown to support various pairings of permanently bound  $\Phi_0/3$  kinks (antikinks), that interpolate between the two distinct vacuum states of the system at  $x = \pm\infty$  (i.e. in the two JJ end triangles of the prism). In a given JJ end triangle, the two vacuum states correspond to plus or minus circulating currents  $J = J_C \sin(\pm\pi/3)$  around the triangle. Translated to the flattened prism of Fig. 1, this implies imposing an external flux of  $\Phi_{q,i} = \Phi_0/3$ , where the flux quantum  $\Phi_0 = h/2e$ . The two vacuum states of the system correspond to a clockwise

circulating current in the left (right) triangle and no circulating current in the right (left) triangle. In a suitably modified system, these two states can be taken as the two basis states for a qubit, and can be shown to correspond to the two lowest states ( $|0\rangle \pm |1\rangle/\sqrt{2}$ ) of the Hamiltonian in Eq. (1).

As the qubit just described is close to the one that has been investigated by Mooij and coworkers [5,6], we can apply the results of their investigation on coupling to the environment, coupling to SQUID detectors, and the low inductance limit [7] to the system proposed here. The main difference between the current proposed system and that of Mooij and coworkers is the spatial mapping of the qubit states (which in turn can engender different coupling terms), and the proposed coupling to a Cirac Zoller type bus [8].

## 2. Qubit characteristics

The Hamiltonian for the four cell qubit of Fig. 1 is given by

\* Tel.: +1-781-377-2968; fax: +1-781-235-2717.

*E-mail address:* stanford.yukon@hanscom.af.mil (S.P. Yukon).

REPORT DOCUMENTATION PAGE				Form Approved OMB No. 0704-0188	
<p>The public reporting burden for this collection of information is estimated to average 1 hour per response, including the time for reviewing instructions, searching existing data sources, gathering and maintaining the data needed, and completing and reviewing the collection of information. Send comments regarding this burden estimate or any other aspect of this collection of information, including suggestions for reducing the burden, to Department of Defense, Washington Headquarters Services, Directorate for Information Operations and Reports (0704-0188), 1215 Jefferson Davis Highway, Suite 1204, Arlington, VA 22202-4302. Respondents should be aware that notwithstanding any other provision of law, no person shall be subject to any penalty for failing to comply with a collection of information if it does not display a currently valid OMB control number.</p> <p><b>PLEASE DO NOT RETURN YOUR FORM TO THE ABOVE ADDRESS.</b></p>					
1. REPORT DATE (DD-MM-YYYY) 06-25-2002		2. REPORT TYPE Journal Article		3. DATES COVERED (From - To) 2001	
4. TITLE AND SUBTITLE A multi-Josephson junction qubit.			5a. CONTRACT NUMBER N/A		
			5b. GRANT NUMBER N/A		
			5c. PROGRAM ELEMENT NUMBER 61102F		
6. AUTHOR(S) Stanford P. Yukon			5d. PROJECT NUMBER 2304		
			5e. TASK NUMBER HE		
			5f. WORK UNIT NUMBER 2304HE03		
7. PERFORMING ORGANIZATION NAME(S) AND ADDRESS(ES) Electromagnetic Scattering Branch (AFRL/SNHE) Source Code: 437890 Electromagnetic Technology Division, Sensors Directorate 80 Scott Drive, Hanscom AFB, MA 01731-2909			8. PERFORMING ORGANIZATION REPORT NUMBER N/A		
9. SPONSORING/MONITORING AGENCY NAME(S) AND ADDRESS(ES) Air Force Office of Scientific Research/NM 875 North Randolph Street Arlington, VA 22203			10. SPONSOR/MONITOR'S ACRONYM(S) AFRL-SN-HS		
			11. SPONSOR/MONITOR'S REPORT NUMBER(S) AFRL-SN-HS-JA-2001-0234		
12. DISTRIBUTION/AVAILABILITY STATEMENT APPROVED FOR PUBLIC RELEASE, DISTRIBUTION UNLIMITED.					
13. SUPPLEMENTARY NOTES ESC Public Affairs Clearance #: 01-0234; Published in in "Quantum Computing and Quantum Bits in Mesoscopic Systems", A. J. Leggett, B. Ruggiero, and P. Silvestrini eds. Kluwer Academic Plenum Publishers, NY USA, (2003)					
14. ABSTRACT We have designed a persistent supercurrent multi-Josephson junction (JJ) qubit whose circuit is based on a flattened JJ triangular prism. The Schroedinger equation for the 1D constrained system is equivalent to the Whittaker Hill equation, for which exact solutions have been found [1]. Symmetric or antisymmetric coupling of the qubit to an external magnetic field, will excite only the corresponding symmetric or antisymmetric terms in the Hamiltonian. This specificity allows coupling to a system bus comprised of an LC resonant loop. We indicate how separate buses might be coupled into a larger branching network.					
15. SUBJECT TERMS Josephson junction; Qubit; Triangular qubit gate; Control Z gate					
16. SECURITY CLASSIFICATION OF:			17. LIMITATION OF ABSTRACT	18. NUMBER OF PAGES	19a. NAME OF RESPONSIBLE PERSON
a. REPORT	b. ABSTRACT	c. THIS PAGE			STANFORD P. YUKON
U	U	U	UU	6	19b. TELEPHONE NUMBER (Include area code)

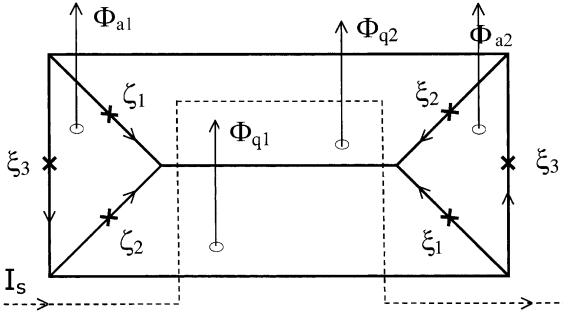


Fig. 1. Circuit diagram of the four cell flattened JJ triangular prism. A three cell variant, with one central cell (corresponding to the opposite prism face with twice the external flux), is also a possible qubit circuit.

$$\begin{aligned}
 H = & 2C(3(\dot{\chi}\Phi_0/2\pi)^2 + (\dot{\theta}\Phi_0/2\pi)^2) \\
 & - 2E_J\{2\cos(\theta)\cos(\phi_r/2)\cos(\phi_q/2) \\
 & \times (\cos(\chi + \phi_a/2) - 2\sin(\theta)\sin(\phi_r/2) \\
 & \times \sin(\phi_q/2)\sin(\chi + \phi_a/2) + \cos(2\chi) \\
 & \times \cos(\phi_s + \phi_q)\}, \quad (1)
 \end{aligned}$$

where we have defined  $\theta = \theta_1 - \phi_r/2$  and  $\chi = \psi_1 + (\phi_q - \phi_a)/2$  with  $\phi_{q,r} = (\phi_{q1} \pm \phi_{q2})/2$  and  $\phi_{q1,2} = 2\pi\Phi_{q1,2}/\Phi_0$ , along with the diagonalizing plus or minus combinations;  $\psi_1 = (\xi_1 - \xi_2)/2$ ,  $\psi_2 = (\xi_1 + \xi_2)/2$ ,  $\theta_1 = (\zeta_1 + \zeta_2)/2$ ,  $\theta_2 = (\zeta_1 + \zeta_2)/2$ , as well as  $\phi_{s,a} = (\phi_{a1} \pm \phi_{a2})/2$  and the zero inductance limit constraint equations  $\{\zeta_1 - \zeta_2 - \zeta_3 = \phi_{a1}$ ,  $\xi_1 - \xi_2 - \xi_3 = \phi_{a2}$ ,  $-\zeta_1 + \zeta_2 = \phi_{q2}$ ,  $\zeta_2 - \zeta_1 = \phi_{q1}\}$ , where  $\phi_{q,s,a} = 2\pi\Phi_{q,s,a}/\Phi_0$  and  $E_J = I_C\Phi_0/2\pi$ . The junction capacitance  $C$  and critical current  $I_C$  have been taken to be equal for all junctions. We require that  $\phi_q = 0$ , otherwise mixing of even and odd  $\chi$  matrix elements can occur upon varying  $\phi_a$ . As a zeroth order Hartree approximation we assume the dynamical variable to be in its ground state, and make the replacement  $\cos(\theta) \rightarrow \langle 0|\cos(\theta)|0\rangle \equiv \eta$  for the  $\chi$  equation of motion, which may then be solved exactly [1]. An harmonic expansion of the  $\theta$  potential around  $\theta = 0$  is then made with  $\cos(\chi) \rightarrow (\langle 0|\cos(\chi)|0\rangle + \langle 1|\cos(\chi)|1\rangle)/2$  to simplify the current calculation. Within this approximation, the Hamiltonian for the variable  $\chi$ , may be written as

$$\begin{aligned}
 H = & M\dot{\chi}^2/2 - 2E_J\{2\langle 0|\cos(\theta)|0\rangle\cos(\phi_r/2) \\
 & \times (\cos(\chi + \phi_a/2) + \cos(2\chi)\cos(\phi_s))\}, \quad (2)
 \end{aligned}$$

where  $M = 6(2C)(\Phi_0/2\pi)^2$ . Replacing  $p_\chi = M\dot{\chi}$ , the momentum conjugate to  $\chi$ , with  $-i\hbar\partial/\partial\chi$  then yields the Hamiltonian operator (in units of  $2E_J$ ),

$$\begin{aligned}
 H/(2E_J) = & -\partial^2/\partial\chi^2/2M_\chi - \{2\eta\cos(\phi_r/2) \\
 & \times (\cos(\chi + \phi_a/2) + \cos(2\chi)\cos(\phi_s))\}, \quad (3)
 \end{aligned}$$

where we have written  $M_\chi = (2E_J)M = 3(2E_J)/(4(E_C/2))$ , with  $E_C = e^2/2C$ .

To model the inclusion of rf forcing and couplings to other qubits, we expand the potential in a power series around  $\phi_a^0 = 0$ ,  $\phi_r^0 \neq 0$ , and  $\phi_s^0 \neq 0$ , keeping  $\delta\phi_i$  terms up to second order. The  $\phi_i^0$  and  $\delta\phi_i$  magnetic fields can be supplied by small loops or by control lines:  $\phi_a^0$  and  $\delta\phi_a$  by a vertical line bisecting the qubit,  $\phi_r^0$  by a horizontal bisecting line, and  $\phi_s^0$  and  $\delta\phi_s$  by the dashed line in Fig. 1, which is designed to maintain  $\phi_{q1,2}^0 = 0$  and  $\delta\phi_{q1,2} = 0$ . In the Hilbert subspace spanned by the qubit states  $|0\rangle$  and  $|1\rangle$ , single qubit rotation operators that are first order in the  $\delta\phi_i$  are given in terms of the Pauli spin matrices  $\sigma_x$  and  $\sigma_z$  by:

$$\begin{aligned}
 \mathbf{Z}_s = & -\eta\sin(\phi_s^0)(\langle 0|\cos(2\chi)|0\rangle \\
 & - \langle 1|\cos(2\chi)|1\rangle)(\delta\phi_s + \delta\phi_q)\sigma_z, \quad (4a)
 \end{aligned}$$

$$\mathbf{X}_a = -\eta\cos(\phi_r^0/2)\langle 0|\sin(\chi)|1\rangle\delta\phi_a\sigma_x. \quad (4b)$$

The second-order interaction terms, needed for two qubit gates, are given by

$$\begin{aligned}
 \mathbf{X}_B = & -\eta\sin(\phi_r^0/2)\langle 0|\sin(\chi)|1\rangle(\delta\phi_a\delta\phi_r/2)\sigma_x, \\
 & (5a)
 \end{aligned}$$

$$\begin{aligned}
 \mathbf{X}'_B = & -\eta\sin(\phi_r^0/2)\langle 1|\sin(\chi)|2\rangle(\delta\phi_a\delta\phi_r/2)\sigma'_x, \\
 & (5b)
 \end{aligned}$$

where  $\sigma'_x = (|2\rangle\langle 1| + |1\rangle\langle 2|)$ . Terms proportional to  $\delta\phi_r^2$  will contribute to a small shift in the frequency  $\mathcal{O}(10^{-4}\omega_{LC})$  of the bus oscillator defined below.

### 3. The control Z gate

To couple the qubits, we use an LC resonant oscillator as a system bus, based on the trapped

ion bus scheme of Cirac and Zoller [8,9] (another scheme based on an LC bus using a direct interaction has been described in Ref. [10]). The bus is coupled to each qubit with a gradiometer type coupling shown in Fig. 3, that nulls  $\delta\phi_a$  or  $\delta\phi_s$  single qubit excitations, and any uniform external perturbation into the bus. The operators for flux and charge in the LC oscillator can be written in terms of creation and annihilation operators  $\{\mathbf{a}^+, \mathbf{a}\}$  as [11].

$$\Phi = \sqrt{\hbar L\omega/2}(\mathbf{a} + \mathbf{a}^+), \quad \mathbf{Q} = i\sqrt{\hbar/2L\omega}(\mathbf{a} - \mathbf{a}^+). \quad (6)$$

If there are  $N$  qubits coupled to the bus, and a fraction  $f_q\Phi$  is available for coupling to the qubits, the amount of flux coupled to each qubit  $f_q\Phi/N$  will yield a Jaynes Cummings type [12] interaction terms (5a) and (5b), with  $\delta\phi_r = 2\pi f_q \times (\hbar L\omega/2)^{1/2}(\mathbf{a} + \mathbf{a}^+)/N\Phi_0$ . The bus frequency  $\omega_{LC}$  is chosen so that neither resonant pulse frequency  $\omega_a = \omega_{10} - \omega_{LC}$  or  $\omega_b = \omega_{21} - \omega_{LC}$ , where  $\hbar\omega_{ij}$  is the energy needed for a transition from level  $j$  to  $i$ , is close to a qubit or bus transition. Solving the Schrödinger eigenvalue equation (3), assuming  $\phi_a^0 = 0$ ,  $\phi_s^0 = \phi_r^0$ ,  $r = -\cos(\phi_s^0)/\cos(\phi_r^0/2) = 0.77$ , and  $(2E_j)/\hbar = 200$  GHz yields  $\omega_{10}/2\pi = 1.553$  GHz,  $\omega_{21}/2\pi = 15.09$  GHz, and one possible choice of  $\omega_{LC}/2\pi = 11.5$  GHz. If the area of the bus coupled to each qubit cell is taken to be  $A = 1 \mu^2$ , the bus inductance for  $f_q \approx 1$  can be approximated by  $L \approx 2N1.25\mu_0\sqrt{A} = N\pi$  pH. The amplitude of the bus oscillator is then  $\Phi_B \approx 1.67 \times 10^{-3}\Phi_0\sqrt{N}$ . For  $r = 0.77$ , the product  $\sin(\phi_r^0)\langle 1|\sin(\chi)|2\rangle/2 = 0.13$ . Assuming  $\delta\phi_a = 2\pi(0.02\Phi_0)/\Phi_0$ , and  $f_q = 1$ , yields a total  $\mathbf{X}'_B$  amplitude of  $1.7 \times 10^{-4}/\sqrt{N}$  and a Rabi frequency of  $\nu_R = 34.3$  MHz/ $N^{1/2}$  for the slowest ( $\mathbf{X}'_B$ ) transition.

#### 4. Sources of decoherence

We defer a detailed discussion of decoherence, but mention that in addition to sources discussed in Refs. [5,6], the bus presents a new source. It can act as a linear array of  $2N$  small  $1 \mu^2$  loop antennas with an RF current amplitude of  $i_{RF} \approx \Phi_B/L \approx 1.1 \times 10^{-7}$  A for  $N = 100$ , yielding a decoherence time from radiation losses of  $\sim 50$  s.

For a substrate refractive index of  $n \approx 3$ , the maximum size of a bus path is  $\sim \lambda_s/10 \sim 870 \mu$ , where  $\lambda_s = \lambda/n$ . A  $\lambda_s/20$  square branching structure with 100 qubits would allow the qubits to be  $\sim 48 \mu$  apart. While the large RF  $\delta\phi_a$  excitation needed for two qubit gates should not enter the bus due to geometric cancellation, its mutual inductance effect on a neighboring ( $48 \mu$  away) qubit is to excite a  $\mathbf{Z}_s$  gate with a Rabi frequency of  $\sim 500$  Hz. Reducing  $N$  to 50 and orienting alternate qubits to be mutually perpendicular could improve this by a factor of  $\sim 10^{-2}$ .

#### 5. Rabi resonant pulse sequence for two qubit gates

The complete sequence of Rabi resonant pulses for a CZ gate, following the presentation in Ref. [9], is shown in Fig. 2. The notation  $\mathbf{X}_{B,m}^\pi(\omega_a)$  signifies an  $\mathbf{X}_B$  gate pulse of  $\pi$  frequency  $\omega_a$  (defined above) acting concomitantly on the bus and the  $m$ th qubit. The sequence of  $\mathbf{X}_B$  and  $\mathbf{X}'_B$  gates in Fig. 2 has been successfully modeled using the subset of 24 basis states  $|m, n; j_{bus}\rangle$  with  $m = \{0, 1, 2\}$ ,  $n = \{0, 1, 2, 3\}$ ,  $j_{bus} = \{0, 1\}$  and the system parameters discussed above.

As the number of qubits on a given bus is limited, we consider connecting a group of buses in an open branching network. This may be accomplished, as shown in Fig. 3, by distinguishing the qubit that connects two buses, and assigning it the sole task of transferring the excitation from the first bus to the second and vice versa. To carry out a CZ gate connecting the  $m$ th qubit on bus #1 with the  $n$ th qubit on bus #2, the first two gates of Fig. 2 are carried out as indicated. The next gate  $\mathbf{X}_{B,t}^\pi(\omega_{10} - \omega_{LC1})$  transfers the excitation on bus #1 to the  $|1\rangle$  state of the transfer qubit. A second  $\mathbf{X}_{B,t}^\pi$  transfers the excitation from the  $|1\rangle$  state of the transfer qubit to bus #2 with excitation frequency  $\omega_{10} - \omega_{LC2}$ . The third gate in Fig. 2 is carried out but with bus #2 excitations and the  $n$ th qubit on bus #2. The final step transfers the bus #2 excitation back to the original bus by reversing the two original  $\mathbf{X}_{B,t}^\pi$  gates. The sign change from the round trip due to the transfer qubit is  $(-i)^4 = 1$ . Since it has been proved [9] that the combination of one qubit gates and the CZ gate is sufficient for

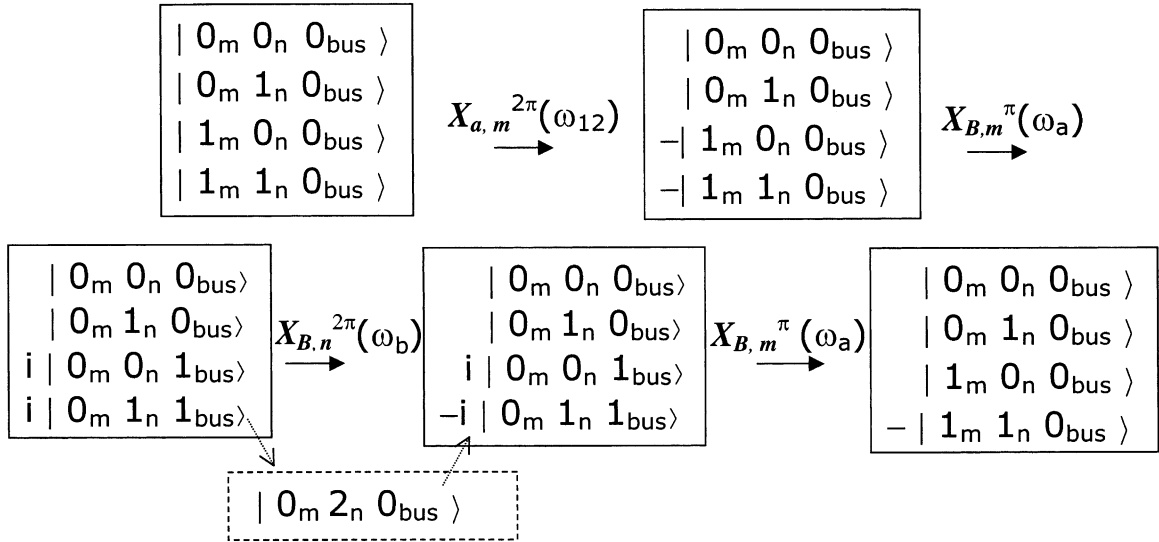


Fig. 2. Gate sequence for the two qubit CZ gate.

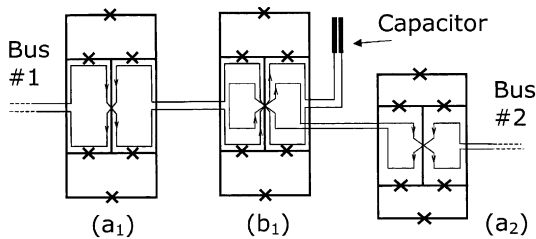


Fig. 3. Circuit detail for the coupling of two resonant LC buses showing a transfer qubit ( $b_1$ ) and computational qubits ( $a_1$ ) on bus #1 and ( $a_2$ ) on bus #2.

producing an arbitrary unitary transform, we have demonstrated that the coupled bus system gates are sufficient for a branched network quantum computer.

### Acknowledgements

The author appreciates helpful conversations with Alexey Ustinov, Jeffrey Yezpez, Farrukh Abdumalikov, Lilli Caputo, and John Derov. This work was carried out with support from Air Force Office of Scientific Research AFOSR.

### References

- [1] K.M. Unwin, F.M. Arscott, Proc. Roy. Soc. Edinb. 71 (1971) 28.
- [2] S.P. Yukon, N.C.H. Lin, IEEE Trans. Mag. 27 (1991) 2736.
- [3] S.P. Yukon, N.C.H. Lin, Nonlinear Superconducting Devices and High  $T_c$  Materials, World Scientific, Singapore, 1994 (p. 137).
- [4] G. Carapella, G. Costabile, P. Sabatino, Phys. Rev. B 59 (1999) 14040.
- [5] J.E. Mooij, T.P. Orlando, L. Levitov, L. Tian, C.H. van der Wal, S. Lloyd, Science 285 (1999) 1036; T.P. Orlando, J.E. Mooij, L. Tian, C.H. van der Wal, L.S. Levitov, S. Lloyd, J.J. Mazo, Phys. Rev. B 60 (1999) 15,398.
- [6] C.H. van der Wal, A.C.J. ter Haar, F.K. Wilhelm, R.N. Schouten, C.J.P.M. Harmans, T.P. Orlando, S. Lloyd, J.E. Mooij, Science 290 (2000) 773.
- [7] D.S. Crankshaw, T.P. Orlando, IEEE Trans. Appl. Supercond. 11 (2001) 1006.
- [8] J.I. Cirac, P. Zoller, Phys. Rev. Lett. 74 (1995) 4091.
- [9] G.P. Berman, G.D. Doolen, R. Mainieri, V.I. Tsifrinovich, Introduction to Quantum Computers, World Scientific, Singapore, 1998.
- [10] Y. Makhlin, G. Schön, A. Shnirman, J. Low Temp. Phys. 118 (2000) 751.
- [11] Z.M. Zhang, L.S. He, S.K. Zhou, Phys. Lett. A 244 (1998) 196.
- [12] P. Meystre, M. Sargent, Elements of Quantum Optics, Springer, Berlin, 1999.